by the fact that despite the smallness of the elastic loading amplitude in comparison with the wave amplitude, it has a substantial effect on the wave profile (Fig. 2). Figure 2 also shows clearly the dynamics of formation and evolution of the elastic foreshock and load at the following distances from the boundaries εy = 0, 0.206, 0.488, 0.862, 1.33, 1.9, 2.55, and 3.3 (lines 1-8).

The authors are grateful to É. I. Andriankin for supporting the study and for discussing the results.

LITERATURE CITED

1. Ya. B. Zel'dovich and Yu. P. Raizer, Physics of Shock Waves and High-Temperature Hydrodynamic Effects [in Russian], Nauka, Moscow (1966).
2. S. Leibowitz and A. Sibass,"Examples of dissipative and disperse systems," in: Nonlinear Waves [Russian translation], Mir, Moscow (1977).
3. G. Whitham, Linear and Nonlinear Waves, Academic Press (1974).
4. É. I. Andriankin and A. I. Malkin, "Theory of propagating nonlinear waves," in: Heating and Explosion in the Cosmos and on Earth [in Russian], VAGO, Moscow (1980).
5. Yu. K. Éngel'brekht and U. K. Nigul, Nonlinear Deformation Waves [in Russian], Nauka, Moscow (1981).
6. S. K. Godunov, Elements of Mechanics of Continuous Media [in Russian], Nauka, Moscow (1978).
7. S. K. Godunov and E. I. Romenskii, "Nonstationary equations of the nonlinear theory of elasticity in Eulerian coordinates," Prikl. Mekh. Tekh. Fiz., No. 6 (1972).
8. A. A. Deribas, V. F. Nesterenko, et al., "Study of the damping process of shock waves in metals upon loading by contact explosion," Fiz. Goreniya Vzryva, No. 2 (1979).
9. K. P. Stanyukovich (ed.), Explosion Physics [in Russian], Nauka, Moscow (1975).
10. P. C. Jain and M. K. Kadalbajoo, "Invariant embedding method for the solution of coupled Burger's equations," J. Math. Anal. Appl., 72, No. 1 (1979).

ION AND NEUTRAL-PARTICLE KINETICS IN A LOW-PRESSURE DISCHARGE CONTAINING A CLOSED HALL CURRENT

V. K. Kalashnikov and Yu. V. Sanochkin

UDC 533.95

Considerable interest attaches to heavy-particle kinetics in a real bounded system; there are various papers on the kinetics of neutral particles near the wall in a fusion reactor such as [1, 2]. One has to consider heavy-particle kinetics in relation to the boundary layer between a dense cold completely ionized plasma and a negative electrode [3]. As the distribution of the neutral particles near the bounding wall is spatially inhomogeneous in such cases, one has to consider the effects on the ion distribution and in particular on the ion transport in the gas from which the ions are derived. It is also important to consider heavy-particle conservation and dynamics for a low-pressure discharge containing a closed Hall current as used in generating accelerated-ion beams [4]. In that case, one cannot restrict consideration to a single component of the heavy particles. Studies have been made [5, 6] on the kinetics of neutral particles and ions in plasma accelerators with closed drift, but allowance was made only for the ionization (the system of kinetic equations for the heavy components was integrated numerically). However, these studies have neglected the interactions between the ions and the neutral particles, which can be important under certain conditions [7].

The purpose of this study is to examine the kinetics of the heavy particles in a low-pressure discharge having closed drift for the magnetized electrons, with allowance for the burnout of the neutral component because of ionization by electron impact and collisions between ions and neutral particles.

Moscow. Translated from Zhurnal Prikladnoi Mekhaniki i Tekhnicheskoi Fiziki, No. 5, pp. 163-169, September-October, 1986. Original article submitted November 14, 1985.

 0021-8944/86/2705-0784$12.50

Elastic collisions with electrons can be neglected in considering heavy-component dynamics. It is shown below that ion–ion collisions can also be neglected to a first approximation in that case. Therefore, if we are not interested in aspects such as the formation of highly charged ions, excited atoms, etc., the kinetic model corresponds to the physical conditions occurring in actual discharges.

Two types of discharge with closed drift are most widely used in experiments and in technology. One can distinguish a discharge containing an anode layer, in which there is a large positive anode potential drop (anode-layer accelerator ALA), and a discharge with an extended electric field (accelerator with closed drift and extended acceleration zone ACDA). In the first case, the applied potential difference φ_0 is localized on a length l of the order of the Larmor radius for an electron with energy $e\varphi_0$ for an electron temperature in the layer $T_e \sim e\varphi_0$, while in the second, the potential drop occurs over a length determined by the size of the insulating insert between anode and cathode l, while T_e is about 10 eV [4]. Under conditions of practical interest, much of the gas entering through the anode burns up, i.e., in both cases, l is larger than the ionization length:

$$l \geqslant \frac{v_g}{\langle \sigma_i v_e \rangle_0 n} \sim \frac{v_i}{\langle \sigma_i v_e \rangle_0 n_g},$$

where v_g and v_i are the characteristic velocities of the neutral particles and ions; n_g and n are the scale factors for the concentrations of neutral particles and charged ones; and $\langle \sigma_i v_e \rangle_0$ is the characteristic value of the ionization coefficient. The speed of the neutral particles $v_g \sim (T_g/M)^{1/2}$ is determined by the anode temperature, while the speed of the ions $v_i \sim (e\varphi_0/M)^{1/2}$ is governed by the discharge voltage ($v_i \gg v_g$). Under ALA conditions, l is less than the mean free path for ion–neutral-particle collisions, whereas the two are of the same order in ACDA:

$$l \leqslant \frac{v_g}{\langle \sigma v_i \rangle n} \sim \frac{1}{\sigma n_g} \tag{1}$$

(σ is the cross section for resonant charge transfer). The neutral particles can be considered to move in free-molecular mode, since $l < (\sigma_g n_g)^{-1}$ (σ_g is the gas-kinetic cross section of the atom). In a low-pressure discharge, one can neglect bulk recombination, and such a discharge is usually employed in an accelerator flow system. The gas enters through the anode, and the ions and the remaining neutral particles leave the discharge gap freely. By virtue of (1), one can neglect the second and subsequent charge transfers, as well as ionization of the fast neutral particles, as will be evident from what follows. If we neglect v_g by comparison with v_i in the equation for the ions (the strong-field approximation), one can assume that the ions formed by charge transfer from slow neutral particles will have zero velocity. One naturally represents the distribution for the neutral particles as $f = f_s + f_f$, where f_s and f_f describe the group of slow particles ($v \approx v_g$) and the fast ones ($v \approx v_i$). The initial system of kinetic equations is

$$v\frac{\partial F}{\partial x} + \frac{eE(x)}{M}\frac{\partial F}{\partial v} = [\nu(x) + \psi(x)]\, n_s(x)\,\delta(v) - |v|\,\sigma(|v|)\, n_s(x)\, F, \tag{2}$$

$$v\frac{\partial f_s}{\partial x} = -[\nu(x) + \psi(x)]\, f_s, \quad v\frac{\partial f_f}{\partial x} = |v|\,\sigma(|v|)\, n_s(x)\, F.$$

Here F is the ion distribution, n_s is the concentration of slow atoms, $\nu = \langle \sigma_i v_e \rangle n_e$ is the electron ionization function, and $\psi = \int |v|\sigma(|v|)F(x, v)dv = \langle \sigma v_i \rangle n_i$. Boundary conditions are specified at the anode:

$$F(0, v) = F_0(v),\ f_s(0, v) = f_{s0}(v),\ f_f(0, v) = 0. \tag{3}$$

The equation for the ions can be solved by the characteristic method. We write the solution to (2) and (3) as

$$F(x, v) = F_0\left(\sqrt{v^2 - v_{0x}^2}\right) \exp\left\{-\int_0^x n_n(y)\,\sigma\left(\sqrt{v^2 + v_{xy}^2}\right) dy\right\} + \tag{4}$$

$$+ \frac{M n_s(z)}{eE(z)}[\nu(z) + \psi(z)][\Theta(v) - \Theta(v - v_{0x})] \times$$

$$\times \exp\left\{-\int_z^x n_s(y)\,\sigma\left(\sqrt{v^2+v_{xy}^2}\right)dy\right\}, \tag{4}$$

$$f_s(x, v) = f_{s0}(v)\exp\left\{-\frac{1}{v}\int_0^x [\nu(x') + \psi(x')]\,dx'\right\},$$

$$f_f(x, v) = \sigma(|v|)\int_0^x n_s(x')\,F(x', v)\,dx'.$$

The argument of z(x, v) in (4) is found from the characteristic equation

$$Mv^2/2e + \varphi(x) = \varphi(z).$$

The symbols used in (4) are

$$v_{xy} \equiv v(x, y) = \sqrt{\frac{2e}{M}[\varphi(x) - \varphi(y)]}, \quad \Theta(v) = \begin{cases} 1, & v > 0, \\ 0, & v < 0, \end{cases}$$

where v_{xy} is the velocity of an ion formed at point x with zero velocity, which it has at point y. According to (4), the solution is defined if n_s and ψ are known and the external conditions are given: the electric-field distribution, the type of gas, and the ionization function. The equations for $n_s(x)$ and $\psi(x)$ follow from (4). For simplicity we put $f_{s0} = n_g\delta(v - v_g)$, and then

$$n_s(x) = n_g \exp\left\{-\frac{1}{v_g}\int_0^x [\nu(x') + \psi(x')]\,dx'\right\}, \tag{5}$$

$$\psi(x) = \psi_0 + \int_0^x \sigma(v_{xy})\,n_s(y)\,[\nu(y) + \psi(y)]\exp\left\{-\int_y^x n_s(z)\,\sigma(v_{yz})\,dz\right\}dy,$$

$$\psi_0(x) = \int v\sigma(|v|)\,F_0\left(\sqrt{v^2 - v_{0x}^2}\right)\exp\left\{-\int_0^x n_s(y)\,\sigma\left(\sqrt{v^2+v_{xy}^2}\right)dy\right\}dv.$$

Then the problem of (2) and (3) amounts to solving two one-dimensional inhomogeneous integral Volterra equations as in (5), which is possible in explicit form in limiting cases. We restrict ourselves in what follows to the case where the ions are formed in the bulk, i.e., $F_0(v) = 0$, and then all the moments of the distributions in (4) can be represented as a series of integrals of the same type. For example, the expressions are as follows for the particle concentrations and the corresponding fluxes:

$$n_i(x) = \int_0^x \frac{n_s(y)\,[\nu(y) + \psi(y)]}{v(y, x)}\exp\left\{-\int_y^x n_s(z)\,\sigma(v_{yz})\,dz\right\}dy, \tag{6}$$

$$n_f(x) = \int_0^x n_s(x')\,dx'\int_0^{x'} \frac{n_s(y)\,[\nu(y) + \psi(y)]}{v(y, x')}\exp\left\{-\int_y^{x'} n_s(z)\,\sigma(v_{yz})\,dz\right\}dy,$$

$$j_i(x) = \int_0^x n_s(y)\,[\nu(y) + \psi(y)]\exp\left\{-\int_y^x n_s(z)\,\sigma(v_{yz})\,dz\right\}dy,$$

$$q_f(x) = \int_0^x n_s(x')\,dx'\int_0^{x'} n_s(y)\,[\nu(y) + \psi(y)]\exp\left\{-\int_y^{x'} n_s(z)\,\sigma(v_{yz})\,dz\right\}dy.$$

The following dimensionless quantities and scale factors are used:

$$x' = \frac{x}{l}, \quad \varphi' = \frac{\varphi}{\varphi_0}, \quad n_i' = \frac{n_i}{n}, \quad n_{s,f}' = \frac{n_{s,f}}{n_g}, \quad v' = \frac{v}{v_i}, \quad \nu' = \frac{\nu}{\nu_0},$$

$$\psi' = \frac{\psi}{\psi_0}, \quad \sigma' = \frac{\sigma}{\sigma_0}, \quad n = \frac{q_0}{v_i}, \quad \nu_0 = \langle\sigma_i v_e\rangle_0\, n, \quad \psi_0 = \nu_0\sigma_0 n_g l, \quad v_i = (2e\varphi_0/M)^{1/2},$$

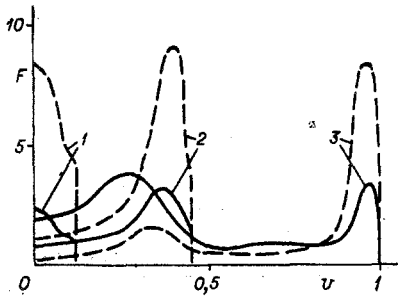

Fig. 1

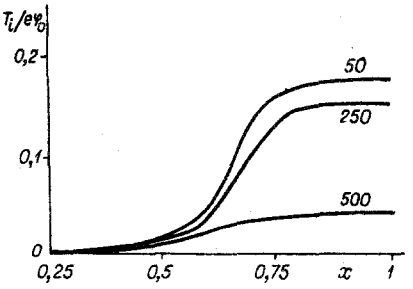

Fig. 2

where $q_0 = n_g v_g$ is the flow rate and σ_0 is the characteristic charge-transfer cross section (the primes are subsequently omitted).

System (5) is written in dimensionless form as

$$n_s(x) = \exp\left\{-I\int_0^x [\nu(x') + \Pi\psi(x')]\,dx'\right\}, \tag{5'}$$

$$\psi(x) = \int_0^x n_s(y)\,\sigma(v_{yx})\,[\nu(y) + \Pi\psi(y)]\exp\left\{-\Pi\int_y^x n_s(z)\,\sigma(v_{yz})\,dz\right\}dy,$$

$$I = \frac{l\langle\sigma_i v_e\rangle_0 n_g}{v_i}, \quad \Pi = \sigma_0 n_g l.$$

System (5) contains the two dimensionless parameters I and Π, which are, respectively, the ratio of the channel length to the ionization length and the charge-transfer length, respectively ($I \sim n_g/\sqrt{\varphi_0}$ is proportional to the flow rate and decreases as the electron temperature increases, while $\Pi \sim n_g$). As in (5'), the other moments in (6) are dependent on I and Π, apart from the fast neutral-particle concentration, which is proportional to $N = n/n_g = v_g/v_i \ll 1$.

We now consider the heavy-particle kinetics for the conditions of a discharge in ACDA. In the experiments, the main attention was given to the flow-rate range for the working gas (mainly xenon) q_0 = 30-100 mA/cm² in current units. It is of interest to examine a wider range q_0 = 50-500 mA/cm², which corresponds to $n_g \approx 10^{13}$-10^{14} cm^{-3} at the anode; taking $\sigma_0 \approx 5\cdot10^{-15}$ cm², with l = 4 cm and $\varphi_0 \approx$ 150 V, we readily get I = 3-30, Π = 0.3-3; to simplify the calculations, the charge-transfer cross section was taken as constant. The observed profiles for the ionization function and potential as used in the calculations are known for q_0 = 50 mA/cm² from [8].

Figure 1 shows the dimensionless ion-velocity distribution in the sections x = 0.2, 0.6, 1 (lines 1-3) for q_0 = 50 and 250 mA/cm² (solid and dashed curves). This is clearly markedly inhomogeneous in x and has two peaks in v near the cathode. At the cathode, there are two groups of particles having substantially different mean velocities, which is due to the specific and almost stepwise change in potential along the discharge gap and the corresponding ionization distribution [8]. The fast group of ions produces the peak at $v \approx 1$ and is generated near the anode.

This peak is relatively small for q_0 = 50 mA/cm² because of the low ionization rate in the anode part. The second group of ions is more numerous at this flow rate and is generated in the region of the potential step, the velocities being less directional. The slow-atom concentration is given by (5') as being exponentially dependent on the flow rate. Therefore, as the flow rate increases, so does the consumption of neutral particles in the anode region, and the peak determined by the fast group, which appears in the one-dimensional treatment, increases. It is difficult and uncertain to calculate $\nu(x)$ for the region adjoining the anode from the experimental data; the ion generation and the electric field are small in this region, and the ions mainly move to the wall and the x direction is not a prominent one [8]. Therefore, the second peak in the ion distribution may be smoothed out or entirely lacking in a real two-dimensional system such as that of [8].

Figure 2 shows the variation in ion temperature along the gap (the numbers on the curves in Figs. 2, 3, 5, and 6 are the flow rates). Near the anode, where the electric field is

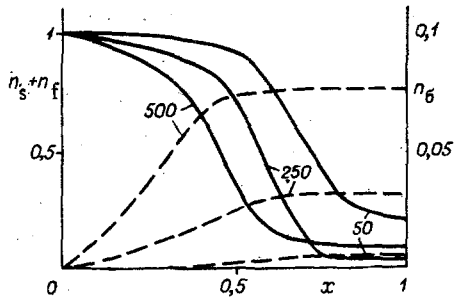

Fig. 3

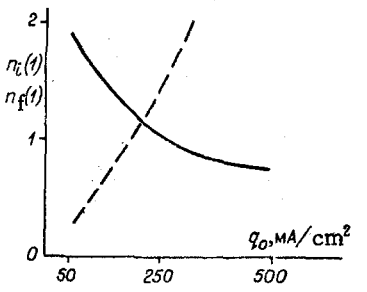

Fig. 4

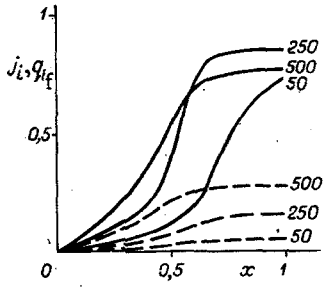

Fig. 5

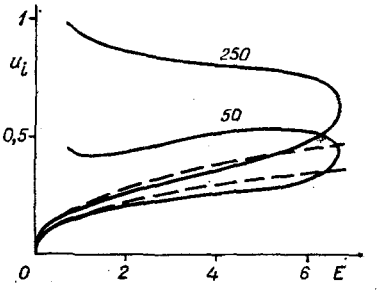

Fig. 6

weak and the concentration of charge particles is low, the ion temperature is low but increases slowly. In the middle of the gap, where the electric fields are strong and there is extensive ionization, T_i increases rapidly and attains about 25 eV in the cathode region for q_0 = 50 mA/cm². As the gas flow increases, the above shift in the main ionization region means that the spread in the ion-flux velocities decreases, and T_i at the cathode is about 7 eV when the flow rate increases by an order of magnitude. These results on the ion heating justify the assumption that one can neglect the Coulomb collisions between ions.

Figure 3 shows the distributions for the total neutral-particle concentration (solid lines) and for the fast neutral particles (dashed lines); it is clear that the type of ionization varies with the flow rate, which explains the behavior of the ion distribution. The ionization and charge transfer at the anode become more rapid as the flow rate increases; the length over which most of the flow becomes ionized tends to decrease. The rapid decrease in the neutral-particle concentration causes a similar deformation in the effective momentum-transfer region. Calculations show that n_s decreases by more than two orders of magnitude in the cathode region when the flow rate increases by an order of magnitude. At the same time, there is a proportional increase in the fast neutral-particle concentration. The range q_0 = 50-500 mA/cm² corresponds to n_f increasing from about 0.005 to 0.08. The change in the relationship between the fluxes of fast and slow neutral particles are such that the total concentration at the exit from the accelerator at first decreases (under these conditions, to about 0.05) and then begins to increase.

Figure 4 shows the concentrations of the charged particles (solid line) and fast neutral particles (dashed line) as functions of flow rate at the exit from the accelerator on an enlarged scale; for $q_0 \simeq 500$ mA/cm², $n_f(1)$ is larger than $n_i(1)$ by about a factor of four. Therefore, this shows that there are always neutral particles in the low-voltage part of a discharge in the range of parameters typical of ACDA, whose concentration is greater than that of the charged particles, i.e., conditions exist for classical electron mobility in the neutral particles.

Figure 5 shows the distributions of the ion flux (solid lines) and the fast neutral-particle flux (dashed lines), which clearly demonstrate the effects of ion–neutral collisions. For q_0 = 500 mA/cm², about 27% of the flow leaves the discharge gap as a flux of fast neutral particles, while the ion flux is correspondingly reduced. However, as the flow rate increases, the increase in the proportion of fast neutral particles becomes slower, and it does not exceed about 30% in this case. Therefore, the neutral particles receive only part of the energy formed by the ions as a result of charge transfer, and the interaction therefore leads to a restricted reworking factor and restricted performance in the accelerating system.

There are no published experimental data for high flow rates, so the profiles for the potential ionization functions were taken as unchanged in the calculations. The results of [9] indicate what conditions correspond to these discharge modes. According to [9], the distributions for the electric field, electron temperature, and electron concentration are determined by the magnetic-field profile, with approximate functional relationships applying between the plasma parameters for given ℓ and φ_0 :

$$E \sim \sqrt{\varepsilon_i \langle \sigma_i v_e \rangle / \langle \sigma_{0e} v_e \rangle}\, H, \quad \varphi_0 \sim H^2 \sqrt{\varepsilon_i}/n_g,$$

$$\langle \sigma_i v_e \rangle / \langle \sigma_{0e} v_e \rangle \sim H^2/n_g^2, \quad n \sim n_g/\sqrt{\varepsilon_i}.$$

Here ε_i is the value of an ion, σ_{0e} is the electron transport cross section, and H is the magnetic field. According to these formulas, if ε_i = const, the electric field E and the ionization function ν remain unchanged if $H \sim \sqrt{q_0}$ increases along with the flow rate, while T_e, which is determined by the ionization coefficient, decreases somewhat. If one incorporates the increase in ε_i as T_e decreases, the electric field can be maintained at the same level with less increase in H. There remains then a weak decreasing dependence of ν on q_0. Consequently, ion–neutral interaction should have even more effect on the results. Under the conditions of an ALA discharge, parameter Π is substantially less than in ACDA under similar conditions. Also, the ionization rate is higher, so the region of effective ion formation is less than the layer thickness, which additionally restricts the scope for momentum and charge exchange between ions and atoms. Therefore, this interaction has only a minor effect on the parameters of the accelerated flux in ALA [10].

Figure 6 shows the dependence of the directional velocity of the ion component on the electric field. Although this model incorporates only single charge transfer, one gets the standard relationship $u_i \sim E^{1/2}$ in the anode region (dashed lines), where $n_i < n_g$. The function u(E) has two values because the electric field is not monotone and has a maximum near the peak in the inhomogeneous magnetic field [8]. These results show that ionization and charge transfer at low flow rates can lead to falls in the speed of the ion flux in some parts of the discharge gap.

LITERATURE CITED

1. S. Rehker and H. Wobig, "A kinetic model for the neutral gas between plasma and wall," Plasma Physics, 15, No. 11 (1973).
2. G. F. Volkov and Yu. L. Igitkhanov, "Kinetics of neutral atoms near the wall of a fusion reactor and impurity formation," Fiz. Plazmy, 3, No. 6 (1977).
3. A. V. Zharinov and Yu. V. Sanochkin, "Heavy-particle dynamics near a negatively charged wall in a dense completely ionized plasma," Fiz. Plazmy, 9, No. 2 (1983).
4. A. I. Morozov, "Plasma accelerators," in: Plasma Accelerators, L. A. Artsimovich (ed.) [in Russian], Mashinostroenie, Moscow (1973).
5. I. V. Melikov, "Calculations on equilibrium flows in plasma accelerators with closed electron drift (ACDA)," Zh. Tekh. Fiz., 44, No. 3 (1974).
6. A. I. Morozov and I. V. Melikov, "Similarities in processes in plasma accelerators with closed electron drift (ACDA) in the presence of ionization," Zh. Tekh. Fiz., 44, No. 3 (1974).
7. V. K. Kalashnikov and Yu. V. Sanochkin, "Heavy-particle kinetics in a low-pressure discharge in a transverse magnetic field," in: Abstracts of the 6th All-Union Conf. on Low-Temperature Plasma Physics [in Russian], Vol. 2, Leningrad (1983).
8. A. M. Bishaev and W. Kim, "A study of the local plasma parameters in an accelerator with closed electron drift and an extended acceleration zone," Zh. Tekh. Fiz., 48, No. 9 (1978).
9. V. K. Kalashnikov and Yu. V. Sanochkin, "The positive column in a low-pressure discharge containing a closed Hall current," Fiz. Plazmy, 11, No. 10 (1985).
10. Yu. S. Popov and Yu. M. Zolotaikin, "Effects of charge transfer on the characteristics of a discharge in a strong transverse magnetic field," Zh. Tekh. Fiz., 41, No. 6 (1971).